

Electrical Characteristics of TMAH-Surface Treated Ni/Au/Al₂O₃/GaN MIS Schottky Structures

M. Siva Pratap Reddy,¹ Jung-Hee Lee,^{2,*} and Ja-Soon Jang^{1,*}

¹Department of Electronic Engineering, LED-IT Fusion Technology Research Center (LIFTRC), Yeungnam University, Gyeongbuk 712-749, Korea

²School of Electrical Engineering and Computer Science, Kyungpook National University, Daegu 702-701, Korea

(received date: 11 December 2013 / accepted date: 21 December 2013 / published date: 10 March 2014)

The electrical characteristics and reverse leakage mechanisms of tetramethylammonium hydroxide (TMAH) surface-treated Ni/Au/Al₂O₃/GaN metal-insulator-semiconductor (MIS) diodes were investigated by using the current-voltage (*I*-*V*) and capacitance-voltage (*C*-*V*) characteristics. The MIS diode was formed on *n*-GaN after etching the AlGaN in the AlGaN/GaN heterostructures. The TMAH-treated MIS diode showed better Schottky characteristics with a lower ideality factor, higher barrier height and lower reverse leakage current compared to the TMAH-free MIS diode. In addition, the TMAH-free MIS diodes exhibited a transition from Poole-Frenkel emission at low voltages to Schottky emission at high voltages, whereas the TMAH-treated MIS diodes showed Schottky emission over the entire voltage range. Reasonable mechanisms for the improved device-performance characteristics in the TMAH-treated MIS diode are discussed in terms of the decreased interface state density or traps associated with an oxide material and the reduced tunneling probability.

Keywords: GaN, Al₂O₃, surface treatment, MIS diode and electrical characteristics

1. INTRODUCTION

The wide-band gap semiconductor, gallium nitride (GaN), has attracted considerable attention because of its potential applications in high-power, high-frequency, and optoelectronic devices.^[1-3] In particular, AlGaN/GaN heterostructures are capable of handling current densities than other *III-V* heterostructures because of the higher two-dimensional electron gas (2DEG) density accumulated at the heterojunction.^[4] In different device structures, GaN metal-insulator-semiconductor (MIS) structures are promising because of the large gate forward voltage swing, small gate leakage current, and surface passivation effect suppressing the drain current collapse.^[5] Recently, using atomic layer deposition (ALD), Al₂O₃ was explored and developed as a gate insulator for GaN MOSFETs and MOS-HEMTs, due mainly to its ability to form normally-off high voltage power switching devices.^[5,6] In MIS structures, acquiring a high-quality insulator, such as Al₂O₃ on a GaN surface, after etching the AlGaN layer in the Schottky region is very critical due to the roughened surface morphology and physical damage caused by plasma etching. This surface morphology and damage can result in the accumulation of crystal defects at the insulator-semiconductor interface, which gives rise to

poor Schottky characteristics of the MIS structures. Therefore, it is important to eliminate the unfavorable effects related to Schottky recess etching.

Tetramethylammonium hydroxide (TMAH), as an alkaline solution, can cause hydrolytic scission and anisotropic etching features compare to other anisotropic solutions, such as KOH, NaOH, CsOH, and NH₄OH.^[7,8] Although TMAH has a lower etch rate, it exhibits outstanding characteristics, such as high selectivity between silicon and their oxide materials without an absence of harmful ions. In particular, TMAH is believed to be a good solution for obtaining a better anisotropic etchant for GaN-based materials.^[8,9] The TMAH treatment is useful for improving the surface roughness, reducing undercutting at convex corners, and removing surface damage caused by plasma etching.

Many researchers have explored a range of metal-insulator-semiconductor schemes for the fabrication of GaN-based MIS devices with different surface treatments.^[10-13] Hashizume *et al.*^[10] examined the defect-related surface states of plasma-exposed *n*-GaN surface by H₂ and N₂ plasma. They reported an anomalous flat portion in the MIS *C*-*V* characteristics for the sample exposed to H₂ plasma. They suggested that a nitrogen-vacancy-related state near the conduction-band edge was introduced to the H₂-plasma-treated GaN surface. No such effects were observed on N₂-plasma-treated GaN surfaces. Qian *et al.*^[11] investigated the enhancement of the performance of Al₂O₃/AlGaN/GaN metal-insulator-semiconductor high electron mobility transistors (MISHEMTs) by a

*Corresponding author: jlee@ee.knu.ac.kr

*Corresponding author: jsjang@ynu.ac.kr

©KIM and Springer

N_2 plasma treatment. They showed that the gate leakage was decreased by two orders of magnitude after pretreating the $Al_2O_3/AlGaN$ interface with N_2 plasma. Lin *et al.*^[12] examined the praseodymium-oxide (Pr_2O_3) passivated $AlGaN/GaN$ MIS-HEMTs with a high dielectric constant, in which the $AlGaN$ Schottky layers were treated with $P_2S_5/(NH_4)_2S_x$ + ultraviolet (UV) illumination. They showed that these surface-treated devices are suitable to low-noise applications. Tsuji *et al.*^[13] used $(NH_4)_2S_x$ and SiH_4 as wet-chemical and plasma treatments on a GaN surface. They reported that the ultra-clean interface of passivation layer and the GaN surface. Previous studies^[14,15] reported that the first is the improvement in the normally-off Al_2O_3/GaN MOSFETs by applying a simple TMAH treatment as a post gate recess etching process, and the second is the influence of a TMAH treatment on the electrical characteristics of $Ni/Au/GaN$ Schottky barrier diodes. The TMAH treatment was found to be quite effective in improving the device-performance characteristics of both devices. However, few studies have examined anisotropic etchant to metal-insulator-GaN contacts. To the best of the authors' knowledge, the TMAH etchant has not been explored as a surface treatment on MIS diodes.

With this aim in mind, in this present work, $Ni/Au/Al_2O_3/GaN$ MIS Schottky structures were fabricated with TMAH treatment and their electrical properties were fabricated using current-voltage ($I-V$) and capacitance-voltage ($C-V$) techniques. The first aim of this study was to compare the Schottky barrier height (Φ_{bo}), ideality factor (n), series resistance (R_s), built-in potential (V_{bi}), and donor concentration (N_D) of TMAH-free and TMAH-treated $Ni/Au/Al_2O_3/GaN$ MIS diodes. The second was to estimate the interface state density (N_{ss}) of the TMAH-free and TMAH-treated $Ni/Au/Al_2O_3/GaN$ MIS diodes. The third was to investigate the carrier transport mechanisms using the reverse $I-V$ characteristics of both MIS diodes.

2. EXPERIMENTAL TECHNIQUE AND ELECTRICAL CHARACTERISTICS

The $AlGaN/GaN$ heterostructure was grown on a sapphire substrate by metal-organic chemical vapor deposition. The structure consisted of a low-temperature (LT) GaN nucleation layer, a 2 μm -thick undoped GaN layer, and a 25 nm-thick $AlGaN$ barrier layer. To fabricate the MIS diode, the active region of the device was isolated by a transformer-coupled-plasma reactive ion etching using a BCl_3/Cl_2 gas mixture. The $AlGaN$ layer in the Schottky region was fully recessed using the same gas mixture. The exposed GaN surface was treated with a TMAH solution at 85°C for 10 min to smooth the surface and remove plasma damage. A 3 nm-thin Al_2O_3 insulator layer was then deposited by ALD on the GaN surfaces after the TMAH treatment. Ohmic contacts were formed by annealing a $Ti/Al/Ni/Au$ (12/200/40/100 nm)

scheme by rapid thermal annealing in a N_2 environment for 30 sec at 850°C. Finally, Schottky contacts were formed by evaporating a Ni/Au (100/120 nm) layer. A TMAH-free $Ni/Au/Al_2O_3/GaN$ MIS diode was also fabricated for comparison. A precision semiconductor parameter analyzer (Agilent-4155 C) and a precision LCR meter (Agilent-4248 A) were used to carry out the electrical measurements.

The diode parameters can be extracted from the thermionic emission (TE) mechanism using the following equation:^[16,17]

$$I = I_o \exp\left(\frac{q(V - IR_S)}{nkT}\right) \left[1 - \exp\left(\frac{q(V - IR_S)}{kT}\right) \right] \quad (1)$$

where I_o is the saturation current density derived from the straight line of $\ln(I)$ at $V=0$, which is expressed as $I_o = AA^*T^2 \exp[-q\Phi_{bo}/kT]$, where q is the electron charge, k is the Boltzmann constant, A is the contact area, A^* is the Richardson constant ($26.4 \text{ A cm}^{-2}\text{K}^{-2}$), T is the temperature, and Φ_{bo} is the Schottky barrier height. Φ_{bo} can be evaluated using the following equation:

$$\Phi_{bo}^{I-V} = \frac{kT}{q} \ln\left(\frac{AA^*T^2}{I_o}\right), \quad (2a)$$

and the ideality factor can be given by

$$n = \frac{q}{kT} \left(\frac{dV}{d \ln I} \right). \quad (2b)$$

The capacitance per unit area, C , of a Schottky diode under a reverse bias V_R is given by the depletion capacitance^[18]

$$\frac{1}{C^2} = \frac{2(V_R + V_{bi})}{q\epsilon_s N_D A^2} \quad (3)$$

where V_R is the reverse bias voltage, V_{bi} is the built-in potential, and N_D is the doping concentration. The diffusion potential or built-in potential is normally measured by extrapolating the $1/C^2$ vs. V_R plot to the x-axis. The zero-bias barrier height from the $C-V$ measurement is defined as $\Phi_{bo}^{CV} = V_{bi} + kT/q + \Phi_n$, where $\Phi_n = (kT/q)\ln(N_C/N_D)$ is the density of states in the conduction band edge is given by $N_C = 2(2\pi m^* kT/h^2)^{3/2}$, where $m^* = 0.22m_0$, and its value was $2.6 \times 10^{18} \text{ cm}^{-3}$ for GaN at room temperature.^[19]

3. RESULTS AND DISCUSSION

3.1 Current-voltage ($I-V$) characteristics

Figure 1 shows the $I-V$ characteristics of TMAH-free and TMAH-treated $Ni/Au/Al_2O_3/GaN$ MIS diodes measured at room temperature. The inset in Fig. 1(a) presents a schematic cross-sectional diagram of the investigated $Ni/Au/Al_2O_3/GaN$ MIS diode. The red arrow lines shown in the inset is a model of the MIS diodes with/without a TMAH treatment. Using equations (2a) and (2b), the calculated barrier height and ideality factor were 0.74 eV and 1.39 for the TMAH-free, and 0.84 eV and 1.12 for the TMAH-treated MIS

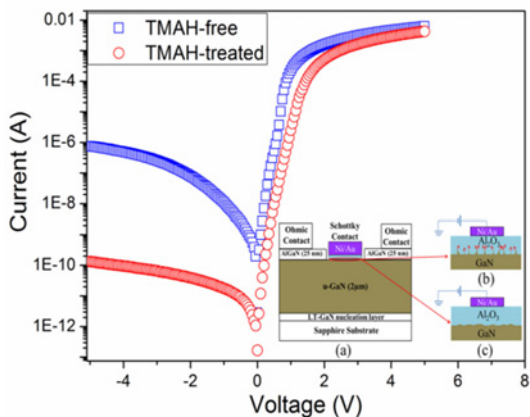


Fig. 1. I - V characteristics plot of the TMAH-free and TMAH-treated Ni/Au/Al₂O₃/GaN MIS diodes at room temperature. The inset shows (a) schematic cross section of the Ni/Au/Al₂O₃/GaN MIS diodes, (b) TMAH-free, and (c) TMAH-treated interface.

diodes, respectively. This suggests that the TMAH treatment affects the increase in barrier height and decrease in the ideality factor. In addition, the TMAH-treated MIS diode has a much lower reverse leakage current than the TMAH-free MIS diode. The increase in barrier height of the MIS diode after the TMAH treatment has two possible explanations. The first explanation was attributed to a decrease in the electron tunneling effect between the TMAH-treated GaN and Al₂O₃. After gate recess etching, sharp protrusions formed on the GaN surface, and the leakage currents at much lower bias voltages were increased by the increased trap-assisted and/or direct tunneling probability of electrons.^[14] Previous investigations^[15] reported that the TMAH treatment after recess etching is quite effective in improving the surface smoothness. Therefore, a smooth surface (after the treatment) causes a decrease in the tunneling effect, and an increase in the overall barrier height.^[20] The second explanation is that the increased barrier height after the TMAH treatment may be associated with increased surface energy band-bending (SEBB) by the effective removal of a plasma-induced surface oxide (Ga_xO_y) on the GaN. Oxide removal means the structural recovery of the etched GaN surface, and the SEBB can be adjusted by normal carriers near the GaN surface instead of oxygen-related defects with an inhomogeneous oxygen composition and occupying deep-level energy states. Eventually, the SEBB is strongly affected by the normal carrier interaction and increases. Therefore, the increased barrier height can be related to the increased SEBB.

From the standpoint of the reduced tunneling probability of electrons, the decrease in the ideality factor for the TMAH-treated MIS diode toward the ideal value of unity can be described well. Basically, the ideality factor for ideal diodes should be unity. On the other hand, low Schottky

barrier height patches caused by a laterally inhomogeneous barrier can exist due to the particular distribution of interface states, the image force effect, recombination-generation, and tunneling^[21,22] in single crystalline semiconductors having some imperfections, and they could be responsible for the higher ideality factor. As an another description, an improvement of the ideality factor for the TMAH-treated MIS diode can be achieved in the reduction of fabrication-induced defects at the interface^[23] and the applying-bias dependence on the barrier height at the real MIS interfaces.^[24]

The ideality factor calculated from the slope of the linear portion of the I - V characteristics includes the effects of the interfacial parameters rather than that of the series resistance. To determine the diode parameters, such an n , Φ_{bo} and R_s , the functions of Cheung method can be obtained as follows:^[25]

$$\frac{dV}{d\ln I} = IR_s + n \left(\frac{kT}{q} \right) \quad (4)$$

$$H(I) = V - \frac{n k T}{q} \ln \left(\frac{I}{A A^* T^2} \right) \quad (5a)$$

and

$$H(I) = n \Phi_{bo} + IR_s \quad (5b)$$

where Φ_{bo} is obtained from data of the downward curvature region in the forward bias I - V plots. Figure 2 show plots of $dV/d\ln I$ vs. I and $H(I)$ vs. I for the TMAH-free MIS diode and TMAH-treated MIS diode, respectively. In the plot of $dV/d\ln I$ vs. I , R_s is the slope and $n k T/q$ is the y-axis intercept using Eq. (4). From Eqs. (5a) and (5b), linear curve fitting of the curve yielded R_s from the slope and Φ_{bo} from the ordinate using the value of the ideality factor obtained from Eq. (2b). From Fig. 2, the values of R_s and n were determined to be 631.86 Ω and 1.41 from the $dV/d\ln I$ vs. I plot (solid square) for the TMAH-free MIS diode. R_s and Φ_{bo} were also calculated to be 621.73 Ω and 0.72 eV from the $H(I)$ vs. I

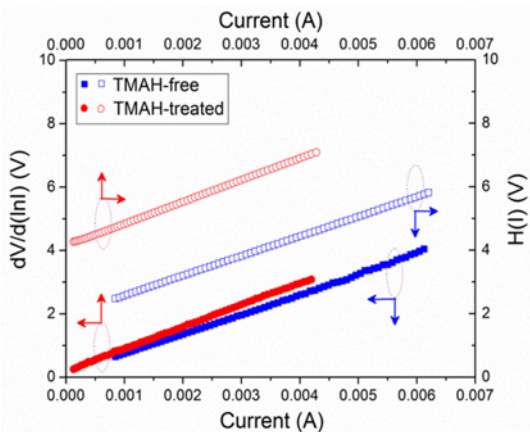


Fig. 2. $dV/d\ln I$ versus I and $H(I)$ versus I plots of TMAH free and TMAH-treated Ni/Au/Al₂O₃/GaN MIS diodes.

plot (open square) of the TMAH-free MIS diode, respectively. The R_s and n of the TMAH-treated MIS diode were $693.04\ \Omega$ and 1.14 using $dV/dlnI$ vs. I plot (solid circle), and $688.57\ \Omega$ and 0.82 eV using the $H(I)$ vs. I plot (open circle), respectively. The parameters obtained from the Cheung method are similar to those from the TE method. The TMAH treatment results in a considerable reduction of the R_s .

3.2 Capacitance-voltage ($C-V$) characteristics

In the $C-V$ measurements, the interface states are unable to respond to the ac signal at a very high frequency (1 MHz). In Fig. 3, to estimate the built-in potential (V_{bi}), the doping concentration (N_D), and barrier height (Φ_{bo}^{CV}), plots of $1/C^2$ vs. V_R were carried out at 1 MHz for the TMAH-free and TMAH-treated MIS diodes. The calculated values of V_{bi} , N_D and Φ_{bo}^{CV} for the TMAH-free MIS diode were determined to be 0.93 V, $4.31 \times 10^{16}\ \text{cm}^{-3}$ and 1.03 eV, respectively. For the TMAH-treated MIS diode, V_{bi} , N_D , and Φ_{bo}^{CV} were found to be 1.05 V, $4.03 \times 10^{16}\ \text{cm}^{-3}$ and 1.16 eV, respectively. The comparisons for both MIS diodes showed that the barrier heights from the $C-V$ method were larger than those from the $I-V$ and Cheung methods. These differences may be associated with a number of factors including the traps in the depletion layer, effective contact area variation, interfacial layer, and charge in surface states.^[22,26] In addition, the apparent decrease in the doping concentration for the TMAH-treated MIS diode might account for invoking interface states in equilibrium with the semiconductor and/or traps associated with the oxide. Table 1 lists the significant parameters of the TMAH-free and TMAH-treated MIS diodes.

3.3 Effect of interface state density (N_{ss})

Using the $C-V$ and $I-V$ measured data, the interface state density (N_{ss}) with respect to the bandgap (E_C-E_{ss}) was

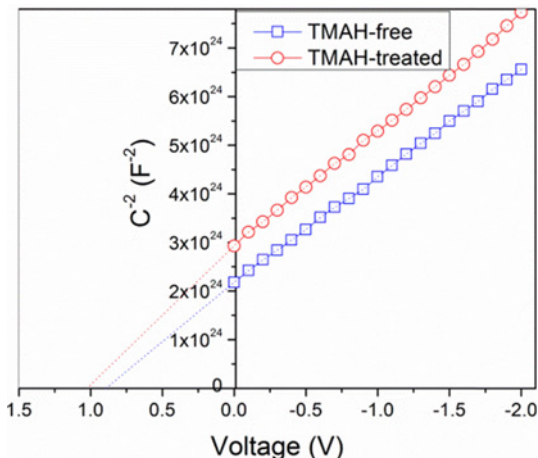


Fig. 3. C^2 versus V plots of TMAH free and TMAH-treated Ni/Au/ $\text{Al}_2\text{O}_3/\text{GaN}$ MIS diodes.

Table 1. Various parameters determined from the $I-V$ and $C-V$ characteristics of TMAH-free and TMAH-treated Ni/Au/ $\text{Al}_2\text{O}_3/\text{GaN}$ MIS diodes.

| Sample | TMAH-free | TMAH-treated |
|--|-----------|--------------|
| $I-V$, Φ_{bo} (eV) | 0.74 | 0.84 |
| Ideality factor (n) | 1.39 | 1.12 |
| $dV/dlnI$, (n) | 1.41 | 1.14 |
| $H(I)$, Φ_{bo} (eV) | 0.72 | 0.82 |
| $dV/dlnI$, R_s (Ω) | 631.86 | 693.04 |
| $H(I)$, R_s (Ω) | 621.73 | 688.57 |
| $C-V$, Φ_{bo} (eV) | 1.03 | 1.16 |
| $N_{ss} \times 10^{12}$ ($\text{eV}^{-1}\text{cm}^{-2}$) | 9.21-0.74 | 1.09-0.13 |

evaluated for the MIS diode using Eq. (6)^[22]

$$N_{ss}(V) = \frac{1}{q} \left[\frac{\varepsilon_i}{\delta} \left((n(V)-1) - \frac{\varepsilon_s}{W_D} \right) \right] \quad (6)$$

where δ is the thickness of the insulator layer (Al_2O_3) and W_D is the depletion layer width that can be obtained from the $1/C^2-V$ measurements at sufficiently high frequency ($f \geq 1$ MHz). The depletion layer thickness was calculated using $W_D = \sqrt{2\varepsilon_s V_{bi}/qN_D}$. The values of ε_i and ε_s for Al_2O_3 layer and GaN were $9.8\varepsilon_0$ and $9.5\varepsilon_0$, respectively. The voltage dependent ideality factor $n(V)$ can be expressed as $n(V) = qV/[kTln(I/I_0)]$. The voltage dependence of the effective barrier height Φ_e is contained in the ideality factor (n) through the following equations:

$$\frac{d\Phi_e}{dV} = \beta = 1 - \frac{1}{n(V)} \quad (7)$$

and

$$\Phi_e = \Phi_b + \beta V \quad (8)$$

where β is the voltage coefficient of Φ_e . Moreover, to consider a MIS diode containing the interface states in equilibrium, the ideality factor becomes greater than unity, as proposed by Card and Rhoderick,^[22] and is given by $n(V) = 1 + \delta/\varepsilon_i[\varepsilon_s/W_D + N_{ss}]$. The energy of the interface states E_{ss} with respect to the bottom of the conduction band edge can be expressed as^[22,27-29]

$$E_C - E_{ss} = q(\Phi_e - V). \quad (9)$$

Figure 4 shows the N_{ss} distribution of the TMAH-free and TMAH-treated MIS diodes below the conduction band ($E_C - E_{ss}$). N_{ss} showed an exponential increase with bias from some above the mid gap towards the top of the conduction band. The magnitude of the N_{ss} , as determined by Terman's method^[30] was $9.21 \times 10^{12}\ \text{eV}^{-1}\text{cm}^{-2}$ ($E_C - 0.24$ eV) to $7.38 \times 10^{11}\ \text{eV}^{-1}\text{cm}^{-2}$ ($E_C - 0.66$ eV) and $1.09 \times 10^{12}\ \text{eV}^{-1}\text{cm}^{-2}$ ($E_C - 0.27$ eV) to $1.25 \times 10^{11}\ \text{eV}^{-1}\text{cm}^{-2}$ ($E_C - 0.79$ eV) for TMAH-free and TMAH-treated MIS diodes, respectively. The TMAH-free MIS diode was approximately one order magnitude higher than the TMAH-treated MIS diode.

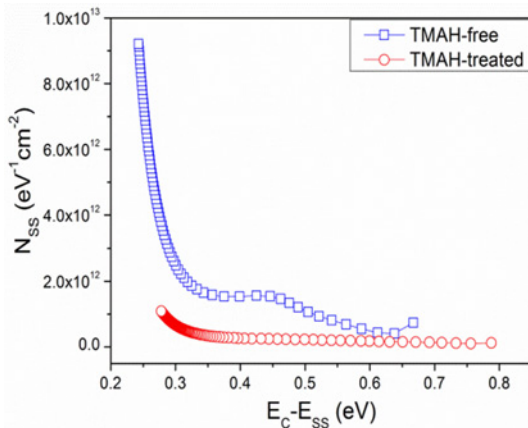


Fig. 4. Density of profiles (N_{ss}) as a function of $E_C - E_{ss}$ TMAH free and TMAH-treated Ni/Au/Al₂O₃/GaN MIS diodes.

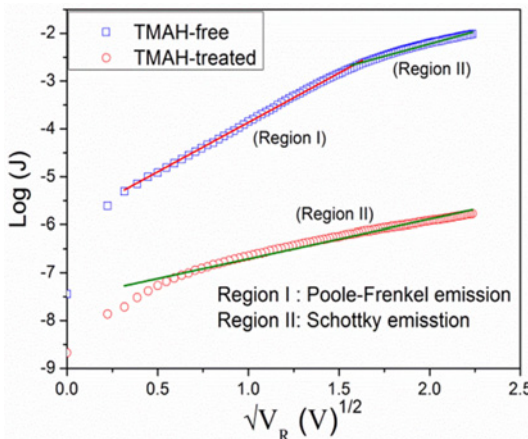


Fig. 5. Plots of $\log(J_R)$ vs. $\sqrt{V_R}$ of TMAH-free and TMAH-treated Ni/Au/Al₂O₃/GaN MIS diodes obtained from the reverse bias $I-V$ characteristics.

Generally, at any specific energy, the N_{ss} of TMAH-free MIS diode was lower than that of the TMAH-treated MIS diode. These behaviors are due mainly to the decrease in deep electronic states existing at the GaN surfaces,^[14,31] the removal of the recess-induced protrusions on the GaN surface^[14] and the unfavorable Ga_xO_y .^[15] Consequently, the N_{ss} of the TMAH-treated MIS diode is reduced significantly.

The reverse bias $I-V$ characteristics of the MIS diodes vary slowly with the applied voltages. The dependency of the reverse current density (J_R) of TMAH-free and TMAH-treated MIS diodes on the reverse bias (V_R) was investigated using Poole-Frenkel and Schottky emission conduction models from the plots of $\log(J_R)$ vs. V_R , as shown in Fig. 5. The reverse current when dominated by Poole-Frenkel emission is given by^[32]

$$J_R = J_0 \exp\left(\frac{S_{PF} V^{1/2}}{k T d^{1/2}}\right) \quad (10a)$$

and the lowering of the Schottky barrier is^[33]

$$J_R = A^* T^2 \exp\left(-\frac{\Phi_{bo}}{kT}\right) \exp\left(\frac{S_{SC} V^{1/2}}{k T d^{1/2}}\right) \quad (10b)$$

where S_{PF} and S_{SC} are the Poole-Frenkel and Schottky field lowering coefficients, respectively. The theoretical value of the S_{PF} ($\beta = 1$) was twice as high as S_{SC} ($\beta = 2$) and can be defined as

$$S_{PF} = S_{SC} = \frac{1}{\beta} \left(\frac{q^3}{\pi \epsilon_0 \epsilon_r} \right)^{1/2}. \quad (11)$$

From Equation (11), the calculated theoretical field lowering coefficients, S_{PF} and S_{SC} , for the TMAH-free and TMAH-treated MIS diodes were 2.42×10^{-5} eVm^{1/2}V^{-1/2} and 1.21×10^{-5} eVm^{1/2}V^{-1/2}, respectively. The comparisons in Fig. 5 show that the conduction of TMAH-free MIS diode is affected by Poole-Frenkel emission at lower voltages (region I) and Schottky emission at higher voltages (region II), whereas the TMAH-treated MIS diode is subject to Schottky emission over the entire voltage region. In particular, considering that Poole-Frenkel emission is closely related to the tunneling of carriers, the better forward and reverse Schottky characteristics for the TMAH-treated MIS diode are directly responsible for the decrease in the interface state density and the reduction in tunneling probability during device operation.

4. CONCLUSIONS

This study examined the electrical characteristics and reverse leakage mechanisms of TMAH-treated Ni/Au/Al₂O₃/GaN MIS diodes by the $I-V$ and $C-V$ characteristics at room temperature. The comparisons showed that the TMAH-treated MIS diode has better Schottky characteristics and a lower reverse leakage current than the MIS diode without the TMAH treatment. The interface state density obtained from the calculations based on the $I-V$ and $C-V$ data is quite sensitive to the surface treatment after a recess etching process. In addition, the TMAH-free MIS diodes exhibit a transition from Poole-Frenkel emission at low voltages to Schottky emission at high voltages, whereas the TMAH-treated MIS diodes show Schottky emission over the entire voltage range. These distinct characteristics could be due to the combined effects of the effective removal of plasma-damage-induced defects during the recess process, the smoothening of the GaN surface, the removal of Ga_xO_y layer, and the decrease in tunneling effects of electrons between Al₂O₃ and surface-treated GaN. These results are expected to be very useful for fabricating high-performance GaN-based electronic devices.

ACKNOWLEDGEMENTS

This study was supported by the MOTIE of Korea through

the industrial infrastructure program under Grant No: 10033630, and the support from a National Research Foundation (NRF) grant through Human Resource Training Project for Regional Innovation.

REFERENCES

1. M. E. Levinshtein, S. L. Rumyantsev, and M. S. Shur, *Properties of Advanced Semiconductor Materials: GaN, AlN, InN, BN, SiC, SiGe*, Wiley, New York (2001).
2. K. J. Lee, M. A. Meitl, J. H. Ahn, J. A. Rogers, R. G. Nuzzo, V. Kumar, and L. Adesida, *J. Appl. Phys.* **100**, 124507 (2006).
3. S. L. Selvaraj and T. Egawa, *Appl. Phys. Lett.* **89**, 193508 (2006).
4. W. Lu, J. Yang, M. A. Khan, and I. Adesida, *IEEE Trans. Electron Devices* **48**, 581 (2001).
5. K. S. Im, J. B. Ha, K. W. Kim, J. S. Lee, D. S. Kim, S. H. Hahm, and J. H. Lee, *IEEE Electron Device Lett.* **31**, 192 (2010).
6. M. Kanamura, T. Ohki, T. Kikkawa, K. Imanishi, T. Imada, A. Yamada, and N. Hara, *IEEE Electron Device Lett.* **31**, 189 (2010).
7. Y. Wu, Y.-I. Lee, L. Wu, and X. Hou, *Microchem. J.* **103**, 105 (2012).
8. J. T. L. Thong, W. K. Choi, and C. W. Chong, *Sens. Actuators A* **63**, 243 (1997).
9. Z. Yang, R. Wang, D. Wang, B. Zhang, K. M. Lau, and K. J. Chen, *Sens. Actuators A* **130-131**, 371 (2006).
10. T. Hashizume and R. Nakasaki, *Appl. Phys. Lett.* **80**, 4564 (2002).
11. F. Qian, T. Yuan, B. Z. Wei, Y. Y. Zheng, N. J. Yu, Z. J. Cheng, H. Yue, and Y. L. An, *Chin. Phys. B* **18**, 3014 (2009).
12. C. W. Lin and H. C. Chiu, *Active Passive Electron. Comp.* **2012**, 459043 (2012).
13. Y. Tsuji, T. Watanabe, K. Nakamura, I. Makabe, K. Nakata, T. Katsuyama, A. Teramoto, Y. Shirai, S. Sugawa, and T. Ohmi, *Phys. Stat. Sol. C* **10**, 1557 (2013).
14. K. W. Kim, S. D. Jung, D. S. Kim, H. S. Kang, K. S. Im, J. J. Oh, J. B. Ha, J. K. Shin, and J. H. Lee, *IEEE Electron Device Lett.* **32**, 1376 (2011).
15. M. S. P. Reddy, D. H. Son, J. H. Lee, J. S. Jang, and V. R. Reddy, *Mater. Chem. Phys.* **143**, 801 (2014).
16. E. H. Rhoderick and R. H. Williams, *Metal-Semiconductor Contacts*, second ed., Clarendon, Oxford (1978).
17. S. Jung, S.-N. Lee, K.-S. Ahn, and H. Kim, *Electron. Mater. Lett.* **9**, 609 (2013).
18. S. M. Sze, *Physics of Semiconductor Devices*, second ed., Wiley, New York (1981).
19. X. J. Wang and L. He, *J. Electron. Mater.* **27**, 1272 (1998).
20. K. Matsumoto, M. Ishii, K. Segawa, Y. Oka, B. J. Vartanian, and J. S. Harris, *Appl. Phys. Lett.* **68**, 34 (1996).
21. S. Altindal, S. Karadeniz, N. Tugluoglu, and A. Tataroglu, *Solid-State Electron.* **47**, 1847 (2003).
22. H. C. Card and E. H. Rhoderick, *J. Phys. D: Appl. Phys.* **4**, 1589 (1971).
23. R. T. Tung, *Phys. Rev. B* **45**, 13509 (1992).
24. H. Cetin, B. Sahin, E. Ayyildiz, and A. Turut, *Physica B* **364**, 133 (2005).
25. S. K. Cheung and N. W. Cheung, *Appl. Phys. Lett.* **49**, 85 (1986).
26. A. M. Goodman, *J. Appl. Phys.* **34**, 329 (1963).
27. A. Singh, K. C. Reinhardt, and W. A. Anderson, *J. Appl. Phys.* **71**, 4788 (1992).
28. M. K. Hudait and S. B. Krupanidhi, *Mater. Sci. Eng. B* **87**, 141 (2001).
29. O. Gullu and A. Turut, *J. Appl. Phys.* **106**, 103717 (2009).
30. L. M. Terman, *Solid-State Electron.* **5**, 285 (1962).
31. S.-H. Jang and J.-S. Jang, *Electron. Mater. Lett.* **9**, 245 (2013).
32. A. S. Riad, *Physica B* **270**, 148 (1999).
33. A. C. Varghese and C. S. Menon, *Eur. Phys. J. B* **47**, 485 (2005).